Sensors and Materials, Vol. 17, No. 1 (2005) 001–006
MYU Tokyo

S & M 0580

Temperature Profiles of Microheaters Using Fluorescence Microthermal Imaging

Edward Van Keuren*, Mark Cheng, Oliver Albertini, Cheng Luo[1], John Currie and Makarand Paranjape

Department of Physics, Georgetown University, Washington, DC, USA
[1]Biomedical Engineering and Institute for Micromanufacturing, Louisiana Tech. University, Ruston, LA 71272, USA

(Received February 9, 2004; accepted October 7, 2004)

Key words: thermal imaging, MEMS, microheaters

A detailed knowledge of the temperature profile is critical in many microelectromechanical systems (MEMS) devices. We used fluorescent microthermal (FMT) imaging for measuring this profile in a MEMS microheater that is an integral part of a glucose-sensing chip. The temperature profile on the heater surface was measured for a range of applied powers below 1 mW. The maximum temperature at the heater center was found to vary linearly with the applied power from room temperature to ~50°C. The imaging was sensitive to temperature changes on the order of 0.1°C. Finite element modeling confirmed both the two-dimensional profile of the temperature on the heater surface as well as the dependence of the temperature on the applied power.

1. Introduction

Microheaters are basic elements of many MEMS devices, such as biomedical[(1)] and gas flow sensors.[(2)] In many of these applications, precise control of the temperature at the heater surface is critical to the device operation. This is of paramount importance when the heating of biological samples is involved. One such example is the bio-flips integrable transdermal (B-FIT) microsystem,[(3)] which is a skin patch glucose sensor that operates by sampling glucose in the interstitial fluid of the skin. This fluid is accessed by the highly controlled thermal microablation of the stratum corneum, or dead skin layer, covering the viable epidermis. For proper operation, the heater performing the ablation must be sufficiently hot to destroy dead skin cells, but not so hot as to damage the living cells

*Corresponding author, e-mail address: vankeu@physics.georgetown.edu

underneath or cause discomfort to the patient.[4] This limits temperatures to roughly less than 50°C. For such a critical application, we have made use of fluorescent microthermal (FMT) imaging techniques to quantify the spatial temperatures at and near the MEMS-based heater. However, this technique can be extended for any application requiring control and monitoring of the temperatures produced by resistive microheating elements.

Determination of the local temperature as a function of applied current is not a trivial measurement. Profiles at temperatures far above ambient have been accurately measured using standard infrared thermal imaging,[5] but little work has appeared in the literature on thermal characterization of microheaters in lower temperatures ranges. In this paper, we demonstrate the imaging of the temperature field using the FMT technique developed by Kolonder and Tyson,[6,7] in combination with modeling and video imaging data. This method has the advantage over other methods, such as IR imaging, of being accurate in the temperature range near and just above room temperature, and it also enables imaging at microscopic lengths scales. The temperature field near the microheaters under evaluation is produced through the application of various current inputs.

In FMT imaging, a dye with a strong temperature-dependent fluorescence emission provides a calibrated measure of local temperature. The dye can be incorporated as a dopant in a sample, such as in a polymer matrix like polymethyl(methacrylate), (PMMA).[8] A number of dyes show a steep drop in fluorescence emission with increasing temperature, usually due to the competition between radiative emission and thermally activated nonradiative decay pathways. This behavior is common in metal organic complexes, in which absorption at UV wavelengths excites the organic ligands, which couple resonantly to the metal ion from which the fluorescence emission originates. At higher temperatures, the coupling of the ligand excited states to other nonradiating states becomes more likely, leading to a decrease in fluorescence. This behavior is well described using Arrhenius type models, and enables the use of these materials as "molecular thermometers." We demonstrate their use here with MEMS microheaters and show not only the efficacy of the method, but also corroboration with modeling data.

2. Materials and Methods

As the temperature-dependent fluorophore, we used the rare earth chelate europium thenoyltrifluoroacetonate (Eu:TTA), commonly used in FMT imaging. This dye possesses a narrow emission band centered on the wavelength 615 nm that displays a strong temperature dependence in the range 0 to 60°C. This band arises from the Eu ion, which is excited by a resonant energy transfer from the organic ligands. This transfer is highly temperature dependent, resulting in good properties for this technique.

For our experiments, the dye was mixed with PMMA in a chloroform solution and cast onto the heater and substrate. Relatively thick films (~100 μm) were used to avoid the interference effects observed in thinner films. Images of the intensity of the fluorescence quantum efficiency[9] or lifetime[10] can then be processed to give two-dimensional temperature maps.

A 1-μm-thick gold microheater, patterned as a meandering resistive element, had 8 μm wide traces separated by a spacing of 8 μm and an overall length of approximately 175 μm.

The microheater sat on top of a 100-μm-thick slab of SU-8, an epoxy polymer used as a photoresist and MEMS structural material, spun onto a glass substrate. The gold was sputter-deposited after a flash deposition of a chrome layer about 100 Å thick which promoted good adhesion of the gold to the substrate. Both the gold and chrome layers were patterned using positive photoresists and wet chemistries for first etching gold, followed by another wet etching process for selectively removing chrome.

Spectral imaging was performed using a FALCON chemical imaging microscope (ChemImage, Inc., Pittsburgh, PA). The fluorescence excitation was provided by a mercury lamp in epi-illumination. Images of the fluorescence emission in the narrow temperature-dependent band around 615 nm were measured using the liquid crystal tunable filter (LCTF) and color CCD camera of the FALCON. The 8 nm bandwidth of the LCTF covers the main part of the narrow temperature-dependent emission of Eu:TTA. Using the empirical formula for the quantum efficiency of emission determined by Barton,[8] a temperature map was generated from the fluorescence emission.

3. Results and Discussion

Figure 1(a) shows a typical raw image of the microheater; Fig. 1(b) shows the corresponding temperature profile for an applied heater power of 0.5 mW. The temperature on the heater surface in this image is roughly 50°C. For fluorescence emission near room temperature, and a pixel value of roughly half the maximum (2048), the smallest change observable is approximately 0.1% of the full scale. Using the calibration given by Barton for Eu:TTA[8], this corresponds to a difference in temperature on the order of 0.05 to 0.1°C. An even higher temperature resolution has been reported for FMT imaging using Eu:TTA[6], but this was not necessary for our application. The range of the method is limited by the temperature-dependent fluorescence of the dye. For temperatures above 60°C, the fluorescence is almost completely quenched, and so the method no longer works.

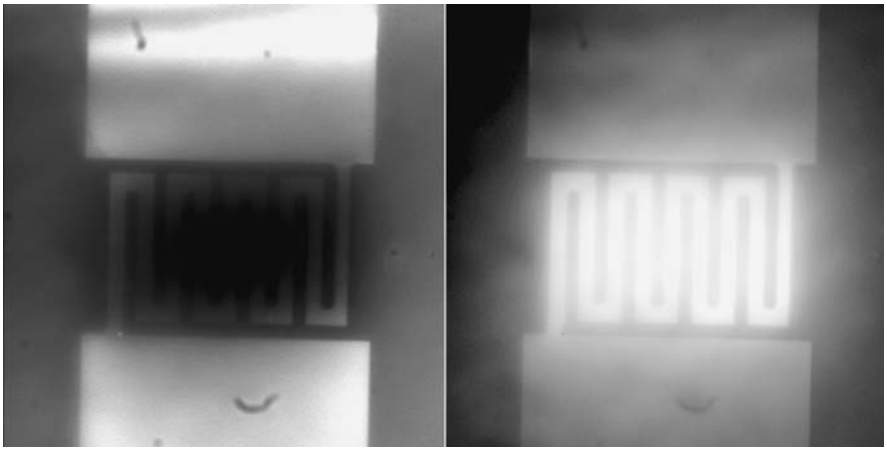

(a) (b)

Fig. 1. A temperature map of the microheater surface at an applied power of 0.5 mW. (a) Raw fluorescence image, (b) temperature profile with pixel intensity proportional to temperature.

One problem encountered was a large variation in emission between separate images. We surmise that this was mainly due to photobleaching of the dye, although there can also be fluctuations in the incident power from the mercury source over time. This effect was minimized somewhat by blocking the incident beam between measurements. We corrected for the variation by normalizing each image with respect to a region that was unaffected by the temperature changes from the heater, i.e., far from the heater center. A second problem, the inhomogeneous distribution of the dye over the sample surface, was corrected by a second normalization using the image at zero applied volts and the measured ambient temperature of 21.5°C. Using this method, the fluorescence decay at each individual pixel relative to room temperature was found, allowing the temperature at each point in the image to be determined independent of the background level. The background will only have an effect on the noise level in the final image, with a room temperature signal near the maximum of the pixel intensity range optimal for achieving the best dynamic range. Care was taken to minimize variations in the coating of the dye-doped polymer which could lead to variations in background, and the gain of the image was adjusted so that the maximum pixel signal was close to the upper limit of the intensity range.

The data showed a roughly linear dependence of the temperature on the input power at low power and a plateau at higher powers. There are two explanations for this leveling off. One is that Eu:TTA has its strongest temperature dependence in the range 0 to 60°C.[8] At higher temperatures, the emission decreased to the noise level, and the method became increasingly inaccurate. In addition, the steady state temperature of the heater depends on the heat conduction in the slab of material underneath the heater as well as on the conduction and convection at the surface of the heater. While the total heat conduction away from the source is linear with temperature, the convective term is not, which could lead to nonlinear behavior in the specific heat of the surface.

We also carried out modeling of the heaters using ANSYS finite element simulation software and compared our data with the modeling results. ANSYS uses a heat balance equation, derived from the principle of the conservation of energy, to find a nodal solution for each finite element that defines the device structure. We employed a steady-state thermal simulation to model the temperature distribution at the heater surface.

Results from a typical ANSYS simulation are shown in Fig. 2. The device shown in the model is 375 μm in length, and the boundaries have been constrained to be at room temperature. The variation in temperature across the heater surface is shown for an applied heater power of 0.24 mW. The temperature profile is similar to the measured results shown in Fig. 1; we are currently performing a more thorough comparison of the two sets of data.

Figure 3 shows the dependence of the surface temperature on the voltage drop across the heater, both the measured values using the FMT imaging and the results of the simulation. Also shown in the figure is a fit to the initial data (below 50°C) of a linear function of the applied power. The measured temperature increase varied roughly linearly with the square of the voltage drop across the heaters, or linearly with the applied power for a constant resistance. In reality, the resistance varies slightly with temperature; however, we assume this effect is not significant in this limited range of temperatures. At higher temperatures, the measured value plateaus. This is likely due to two effects. One is the

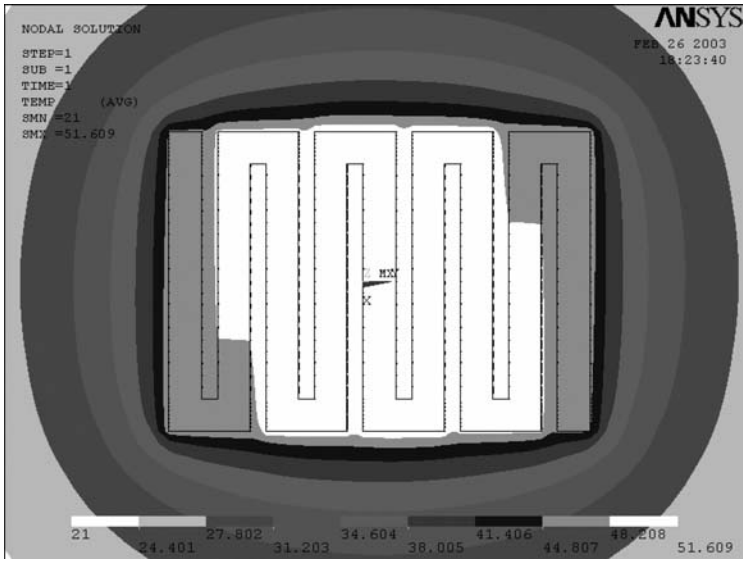

Fig. 2. ANSYS simulation of a microheater element on SU-8 illustrating the thermal gradient in the polymer. The temperature at the heater center is 60°C, the differently shaded areas indicate decreasing temperature in increments of ~8°C to room temperature far from the heater.

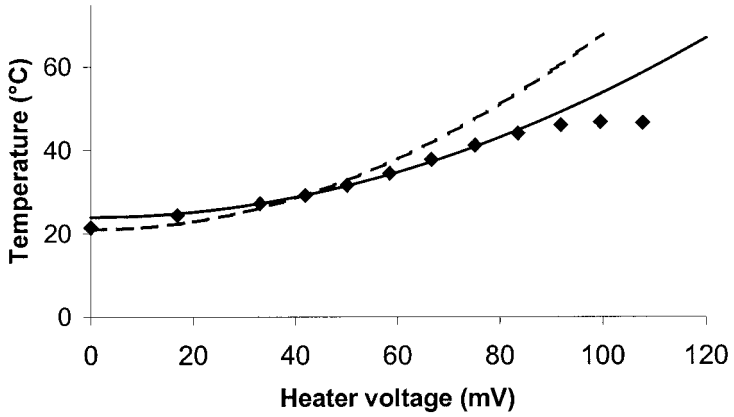

Fig. 3. Plots of the central heater temperature vs. applied power measured using FMT (data points), a second order polynomial fit vs voltage drop (solid line), and from ANSYS simulations (dashed line).

nonlinearity of the heat transfer at higher temperatures — here the convection through the air, as well as nonlinear properties of the heaters and substrate, cause the temperature to deviate from linearity. However, a more significant effect comes from the dye used here.

The drop in fluorescence emission from the temperature-dependent emission band for Eu:TTA drops rapidly to zero at around 60°C, and so the accuracy of the method at these temperatures becomes increasingly poor. This limitation can be easily resolved by using alternative dyes with temperature-dependent emission spectra over higher temperature ranges.

Initially we found that the simulation gave a temperature increase vs applied power about twice the measured value. We refined the simulation by taking into account the thick polymer (PMMA) layer on top of the heaters, which plays a significant role in moderating the temperature increase of the heater. The agreement was then good, supporting the data analysis used for the FMT imaging.

In conclusion, we have demonstrated the use of FMT imaging to characterize surface temperature profiles on MEMS heaters. The accurate characterization enables calibration of the devices for proper functioning and allows models for predicting thermal effects to be refined. The great utility of the method is that it may easily be extended to three dimensions using confocal or two-photon imaging. Our current research involves doing just this, and our results will be reported in full in the near future.

Acknowledgement

This work was supported in part through a BioFlips DARPA-MTO (DAAD19-00-1-0390, Program Manager: Dr. Michael Krihak, and ARO Technical Monitor Dr. Robert Campbell).

References

1 M. Paranjape, J. Garra, S. Brida, T. Schneider, R. White and J. Currie: Technical Digest, Solid-State Sensor, Actuator and Microsystem Workshop, 2002 (Hilton Head Island, South Carolina, 2002) p. 73.
2 A. Vasiliev, S. Gogish-Klushin, D. Kharitonov, A. Pisliakov, V. Pevgov and M. Paranjape: Technical Digest (CD) Eurosensors '02, (Prague, 2002) p. 248.
3 M. Paranjape, J. Garra, S. Brida, T. Schneider, R. White and J. Currie: Sensors and Actuators A **104** (2003) 195.
4 E. Van Keuren, J. Currie, M. Nelson, M. Paranjape, T. Schneider, R. Smith, P. Treado, J. Ward and R. White: Mat. Res. Soc. Symp. Proc. **687** (2002) B. 1. 3. 1.
5 M. Gaitan, M. Parameswaran, R. Johnson and R. Chung: SPIE Proc. Infrared Imaging Systems **1969** (1993) 363.
6 P. Kolonder and J. Tyson: Appl. Phys. Lett. **40** (1982) 782.
7 P. Kolonder and J. Tyson: Appl. Phys. Lett. **42** (1983) 117.
8 D. Barton: Proc. 20th Inter. Symp. Testing and Failure Analysis (1994) p. 87.
9 P. Tangyunyong, A. Liang, A. Righter, D. Barton and J. Soden: Proc. 22nd Intern. Symp. Testing and Failure Analysis (Los Angeles, 1996) p. 55.
10 T. Samulski, P. Chopping and B. Haas: Phys. Med. Biol. **27** (1982) 107.